Journal of the Mechanics and Physics of Solids, in press (2018)

Energy of periodic discrete dislocation networks

Nicolas Bertin[a], Wei Cai[a]

[a] *Department of Mechanical Engineering, Stanford University, Stanford, CA, USA*

Abstract

We present an approach to compute the stored energy associated with arbitrary discrete dislocation networks subjected to periodic boundary conditions. To circumvent the issue of conditional convergence while keeping the computational cost tractable, we develop a regularization procedure that involves two equivalent measures of the dislocation network energy. Taking advantage of the non-singular formulation, the energy is first evaluated by explicitly calculating the conditionally convergent sum of all interactions between dislocation segments. Regularization constants are then determined by volume integral of the smooth elastic stress fields produced for large values of the dislocation core radius. The approach is employed to investigate the stored energy of a series of idealized dislocation configurations and large-scale networks generated by discrete dislocation dynamics (DDD) simulations. It is found that (1) the stored energies predicted by DDD simulations are in good agreement with experimental measurements of about 5% of the work done, and (2) Taylor lattice configurations provide surprisingly good energetics models for complex DDD networks, thereby confirming the screening of long-range stresses in work-hardened dislocation structures.

Keywords: Dislocations, Energy, DDD

1. Introduction

Plastic deformation in metals is primarily caused by the motion of dislocations in response to the imposed mechanical loading. While this process is highly irreversible and results in dissipating most of the work done to the crystal into heat, a fraction of the energy remains stored within the crystal in the form of elastic and core energies of the dislocations. The stored energy is of particular interest since it depends both on the density of dislocations and on their arrangement. In addition, it provides the driving force for several phenomena that are important for the microstructure evolution, such as static and dynamic recovery, and recrystallization.

As such, the energy associated with dislocation structures has become a key ingredient in our understanding of plastic deformation, and a fundamental quan-

tity in the theories of work-hardening [1–3]. Specifically, it has long been recognized that the sensitivity of the elastic energy to the geometric arrangements of dislocations provides an opportunity to compare model predictions with experimental measurements. As a result, several efforts have been undertaken early on to measure stored energies at different stages of the deformation during experiments, typically via the use of calorimetry methods (e.g. [4–6]). Concurrently, several thermodynamical models of plasticity that include stored energy as an internal variable have been devised [7, 8], and a few numerical methods have been proposed to compute explicitly the energy of a dislocation network in the context of continuum formulations (e.g. [9, 10]). When dealing with explicit representations of dislocation lines however, no such methods have been proposed, except in [11] where an approach to calculate the energy associated with dislocations from 2D Discrete Dislocation Dynamics (DDD) simulations in confined volumes was developed. More generally, no technique is available for dealing with arbitrary dislocation networks subjected to periodic boundary conditions, e.g. such as those found in bulk 3D DDD simulations, whose ability to generate complex networks that capture salient features of the plastic deformation (e.g. junction formation) has been successfully demonstrated [12, 13].

The lack of energy methods for 3D periodic structures is primarily attributed to the difficulties associated with two distinct convergence issues that arise when dealing with sets of periodic discrete dislocation structures. Firstly, the singularity at the dislocation core in the classical theory of elasticity precludes a direct evaluation of the energy, which is unbounded. As pointed out in [14], the use of a simple cut-off radius within the core region to bypass this difficulty is unsatisfactory as the evaluation of the self-energy becomes inconsistent with the self-force. The problem was addressed using the non-singular formulation in which the Burgers vector is smoothly spread out around the dislocation line [15].

The second issue arises when dealing with periodic dislocation configurations, encountered in bulk DDD simulations subjected to periodic boundary conditions (PBC). For this type of configurations, it can be shown that the direct sum of interaction energies is not absolutely convergent [16]. This behavior implies that, when using a naive approach whereby all interaction energies between lines and their periodic images are summed, the resulting energy depends on the order (or equivalently the truncation scheme) of the summation.

In this paper, we develop an approach to calculate the elastic energy associated with an arbitrary network of discrete dislocations that addresses both the issues mentioned in the above. To this end, we propose to take advantage of the non-singular theory of dislocations [15] and to treat the core width as a numerical parameter, while utilizing the property that the periodic sum of the second derivative of the interaction energies with respect to the core parameter is absolutely convergent. With this, a regularized solution of the network energy can

be obtained by comparing the explicit sum of interaction energies with the value of the energy calculated from volume integrals of the dislocations stress fields, which are conveniently evaluated at very large values of the core radius to control the computational cost.

The rest of the paper is organized as follows. We start by discussing the problem of the conditional convergence in details in section 2. The procedure to regularize the elastic energy is then presented in section 3. In section 4, we demonstrate the validity of the approach by examining the energies of dislocation loops and infinite lines. The approach is then used in section 5 to calculate the stored energies for (i) idealized grain-boundary and Taylor lattice structures, and (ii) a large-scale network generated by DDD simulations. In doing so we find that the Taylor lattice model captures surprisingly well the stored energy associated with strain-hardened dislocation structures. This finding and specific aspects of the approach are further discussed in section 6. A conclusion is given in section 7.

2. Problem statement

2.1. Non-singular elastic energy of a discrete network of dislocations

In principle, the calculation of the elastic energy of a dislocation network can be performed in two equivalent ways. Consider a discretized network of dislocations composed of a set of interconnected dislocation segments. Following the classical approach, the elastic energy of the system can be obtained from the total stress field $\boldsymbol{\sigma}(\boldsymbol{x})$ as:

$$E^{\text{vol}} = \frac{1}{2} \int S_{ijkl}\sigma_{ij}(\boldsymbol{x})\sigma_{kl}(\boldsymbol{x})\, d^3\boldsymbol{x} \tag{1}$$

where S is the elastic compliance tensor, and superscript "vol" is used to indicate that this measure of the elastic energy results from an integral over the material volume. Since the energy in expression (1) is infinite due to the stress singularities of dislocations in the classical theory of elasticity, truncation or regularization procedures are introduced in numerical approaches to eliminate the singular behavior at the dislocation core. In the context of the non-singular dislocation theory [15], the singularity is removed by smoothly spreading out the Burgers vector around dislocation lines. However, even after such treatments, the highly non-linear behavior of the (finite) stress field in the vicinity of dislocation lines still precludes a direct evaluation of the volume integral in equation (1). Since the size of the core is on the order of the Burgers vector magnitude, the resolution required to accurately integrate stress field variations near dislocation cores typically renders the calculation prohibitive even for small dislocation networks.

Alternatively, the energy of the system can be calculated by explicitly summing the contributions of segment interactions. In general, the elastic energy of a network of dislocation lines can be decomposed as:

$$E^{\text{seg}} = E^{\text{self}} + E^{\text{int}} \tag{2}$$

where E^{self} denotes the self-energies of the dislocations, E^{int} accounts for the elastic interaction energies between all pairs of dislocation segments, and superscript "seg" indicates that this decomposition follows from a segment-based approach. When considering all dislocation segments in the network, the total elastic energy can be computed explicitly as:

$$E^{\text{seg}} = \sum_{\alpha} E^{\text{self}}_{\alpha} + \sum_{\alpha} \sum_{\beta > \alpha} E^{\text{int}}_{\alpha\beta} \tag{3}$$

where the self-energy sum is carried over all segments α in the network, and the interaction sum is performed over all distinct segment pairs $\alpha\beta$. Note that the validity of expression (3) entails that the Burgers vector is conserved at each node of the network.

Following the non-singular dislocation theory proposed in [15], the interaction energy between two straight dislocation segments α and β with Burgers vector $\boldsymbol{b}$ and $\boldsymbol{b'}$ in an isotropic elastic medium is expressed as:

$$\begin{aligned} E^{\text{int}}_{\alpha\beta} = &- \frac{\mu}{8\pi} \int_{\boldsymbol{x}^1_\beta}^{\boldsymbol{x}^2_\beta} \int_{\boldsymbol{x}^1_\alpha}^{\boldsymbol{x}^2_\alpha} R_{a,kk} b_i b'_j dx_i dx'_j - \frac{\mu}{4\pi(1-\nu)} \int_{\boldsymbol{x}^1_\beta}^{\boldsymbol{x}^2_\beta} \int_{\boldsymbol{x}^1_\alpha}^{\boldsymbol{x}^2_\alpha} R_{a,ij} b_i b'_j dx_k dx'_k \\ &+ \frac{\mu}{4\pi(1-\nu)} \left(\int_{\boldsymbol{x}^1_\beta}^{\boldsymbol{x}^2_\beta} \int_{\boldsymbol{x}^1_\alpha}^{\boldsymbol{x}^2_\alpha} R_{a,kk} b_i b'_i dx_j dx'_j - \mu \int_{\boldsymbol{x}^1_\beta}^{\boldsymbol{x}^2_\beta} \int_{\boldsymbol{x}^1_\alpha}^{\boldsymbol{x}^2_\alpha} R_{a,kk} b_i b'_j dx_j dx'_i \right) \end{aligned} \tag{4}$$

where $R_{a,ij} = \partial^2 R_a / \partial x_i \partial x_j$ denotes second derivative of the non-singular radius vector (see Appendix A), $\boldsymbol{x}^i_\alpha$ and $\boldsymbol{x}^i_\beta$ $(i = 1, 2)$ specify the coordinates of the segments end points, and μ and ν are the shear modulus and Poisson's ratio, respectively. Thanks to its non-singular nature, an analytical expression for equation (4) can be conveniently obtained [15]. Note that the self-energy E^{self}_{α} of a dislocation segment is directly obtained as a special case of expression (4) when $\alpha = \beta$. From expression (4), it also follows that the interaction energy $E^{\text{int}}_{\alpha\beta} = E^{\text{int}}_{\alpha\beta}(\boldsymbol{R}_{\alpha\beta}, a)$ is a function of the radius vector $\boldsymbol{R}_{\alpha\beta}$ linking the coordinates spanning segments α and β, and of the core radius a of the isotropic Burgers vector spreading function [15].

We note here that, in the context of the non-singular formulation, the two measures of the elastic energy in equations (1) and (3) remain equivalent, and

their value depends on the choice of the core radius a. Clearly, the physical energy of a dislocation network should not depend on the choice of a numerical parameter. For the sake of clarity however, we will postpone the introduction of a core energy term to eliminate this dependence until section §5.2, in which this additional contribution will be needed to establish relevant comparisons between our calculations and experimental measurements.

2.2. Conditional convergence of the energy in periodic cells

Dislocation networks generated from numerical simulations (e.g. DDD, MD) are often subjected to PBC to mimic the bulk behavior. Under these conditions, the evaluation of the elastic energy of the system suffers from the issue of conditional convergence, as already pointed out in [16].

To illustrate this issue, let us consider an arbitrary dislocation network composed of discrete dislocation segments contained in a primary simulation volume (supercell) of length L_x, L_y, L_z with periodic vectors $\boldsymbol{c}_1, \boldsymbol{c}_2, \boldsymbol{c}_3$. The interaction energy term introduced in the decomposition in equation (3) is obtained by calculating:

$$E^{\text{int}} = \sum_{\alpha} \sum_{\beta > \alpha} \sum_{\boldsymbol{P}} E^{\text{int}}_{\alpha\beta}(\boldsymbol{R}_{\alpha\beta} - \boldsymbol{P}, a) \tag{5}$$

where the outer sums are carried over all dislocation segments α and β contained within the primary volume, and the innermost sum runs over the periodic lattice vectors $\boldsymbol{P} = n_1\boldsymbol{c}_1 + n_2\boldsymbol{c}_2 + n_3\boldsymbol{c}_3$ (n_i are integers) specifying the position of image dislocation segments with respect to their primary counterparts. In practice, the periodic lattice sum in equation (5) is often truncated to a finite number of images $N^{\text{img}} = |n_i|$ in each direction $i \in \{1, 2, 3\}$.

Examining expression (4), it follows that the interaction energy between a pair of elementary dislocation segments behaves as R^{-1} at large R:

$$E^{\text{int}}_{\alpha\beta}(\boldsymbol{R}, a) \propto \frac{1}{R_a} = \frac{1}{\sqrt{R^2 + a^2}} \tag{6}$$

Consequently, the sum of the absolute values of the network interactions energy E^{int} given in equation (5) diverges:

$$\sum_{\boldsymbol{P}} \left| E^{\text{int}}_{\alpha\beta}(\boldsymbol{R}_{\alpha\beta} - \boldsymbol{P}, a) \right| \propto \int^{\infty} dR\, 4\pi R^2 \frac{1}{\sqrt{R^2 + a^2}} \propto \int^{\infty} R dR \sim \infty \tag{7}$$

Equation (7) implies that the result of a naive evaluation of the interactions energy using expression (5) is not absolutely convergent, and will therefore depend on the order (or truncation scheme) of the sum. While equation (7) pertains to dislocation segments, we also point out that the interaction energy between closed

loops behaves as $1/R^3$, and is therefore also conditionally convergent. As a result, the lattice sum (5) must be regularized in order to unambiguously determine the elastic energy of a periodic dislocation network.

3. Regularization of the network energy

In this section, a procedure to regularize the elastic energy of a periodic network of dislocations is presented. From expression (6), we note that the dislocation interaction energy is behaving as $1/R^m$, with $m = 1$. Following the approach proposed in [16], a convenient way to regularize such a quantity consists in finding derivatives to a certain order whose periodic lattice sums are absolutely convergent. The regularized solution is then obtained by integration of the convergent derivatives. In our approach, the integration constants are determined by comparing the segment-based energy measure with the energy obtained by volume integral of the dislocations stress field, thereby providing a unique quantification of the dislocation network energy. This approach therefore requires both energy measures to be regularized, as presented in the following sections.

3.1. Regularization of the analytical energy calculation

In the context of the segment-based energy calculation, we propose to take advantage of the core radius parameter a to regularize the sum in expression (5). More specifically, by denoting $s = a^2$, it immediately follows that

$$\frac{\partial^2 E^{\text{int}}_{\alpha\beta}(\boldsymbol{R}, a)}{\partial s^2} \propto \frac{1}{R^5} \tag{8}$$

at large R, such that the lattice sum of the second derivative of the interaction energy with respect to s,

$$\sum_{\boldsymbol{P}} \left| \frac{\partial^2 E^{\text{int}}_{\alpha\beta}(\boldsymbol{R}_{\alpha\beta} - \boldsymbol{P}, a)}{\partial s^2} \right| \propto \int^{\infty} dR\, 4\pi R^2 \frac{1}{R^5} \propto \int^{\infty} \frac{1}{R^3} dR \tag{9}$$

converges absolutely. (Note that the first derivative of $E^{\text{int}}_{\alpha\beta}(\boldsymbol{R}, a)$ behaves as $1/R^3$ and the lattice sum of its absolute value diverges logarithmically, hence the use of the second derivative.) From a general perspective, relation (9) indicates that the conditional convergence of the interaction energy in equation (5) produces at worst a spurious linear term as a function of s in the evaluation of the total energy, which depends on the order (or truncation scheme) of the lattice sum. Consequently, the periodic sum of the elastic energy in equation (2) for a dislocation network can be written as:

$$
\begin{aligned}
E^{\text{seg}} &= E^{\text{self}} + E^{\text{int}} \\
&= E^{\text{reg}} + E_1 s + E_0
\end{aligned} \tag{10}
$$

where E^{reg} is the regularized energy, and E_1 and E_0 are constants quantifying the linear and constant error terms, respectively. Rearranging equation (10), the unique regularized solution for the network energy is obtained as:

$$
E^{\text{reg}} = E^{\text{seg}} - E_1 a^2 - E_0 \tag{11}
$$

Obtaining the regularized solution (11) is contingent on the evaluation of constants E_1 and E_0. In principle, their evaluation can be achieved by comparing the total elastic energy calculated segment-wise with another measure of the elastic energy.

3.2. Regularization of the stress energy calculation

As presented in equation (1), the total elastic energy of a dislocation network can be alternatively obtained in terms of the dislocations stress field as:

$$
E^{\text{vol}} = \frac{1}{2} \int S_{ijkl} \sigma_{ij}^{\text{reg}}(\boldsymbol{x}) \sigma_{kl}^{\text{reg}}(\boldsymbol{x}) \, d^3\boldsymbol{x} \tag{12}
$$

As pointed out in section 2.1, a direct evaluation of the energy from dislocation stress fields using equation (12) is generally precluded by its high computational cost. However, taking once again advantage of the non-singular theory [15], the computational burden can be greatly alleviated when considering large values of the core radius a. This is because at large values of a, the stress produced by a dislocation segment becomes a smooth field, and therefore requires a much smaller number of integration points to be accurately integrated. Furthermore, since the dependence of the elastic energy of the system on parameter a is known explicitly from relation (11), the linear error constants E_0 and E_1 can be conveniently obtained by having both the segment-based and volume-based measures of the energy in equations (3) and (12), respectively, coincide at large values of a.

Before laying out the complete regularization procedure, it is important to note that the calculation of the elastic energy in equation (12) is also subjected to the issue of conditional convergence when evaluating the stress field, hence the use of the regularized stress field $\boldsymbol{\sigma}^{\text{reg}}(\boldsymbol{x})$ in expression (12). Specifically, the total stress field arising from a set of dislocation segments in a periodic volume can be evaluated at field point $\boldsymbol{x}$ as:

$$
\sigma_{ij}^{\text{tot}}(\boldsymbol{x}) = \sum_{\alpha} \sum_{\boldsymbol{P}} \sigma_{ij}^{\alpha}(\boldsymbol{x} - \boldsymbol{P}) \tag{13}
$$

where σ_{ij}^{α} denotes the (singly-convoluted) non-singular stress field produced by dislocation segment α whose expression is provided in Appendix B, and $\boldsymbol{P} = n_1\boldsymbol{c}_1 + n_2\boldsymbol{c}_2 + n_3\boldsymbol{c}_3$ refers to the set of periodic lattice vectors. Conducting the same analysis as in §2.2, and observing that the stress field produced by an elementary dislocation segment behaves as $1/R^2$ at large R (see Appendix B), it follows that the sum in equation (13) is not absolutely convergent:

$$\sum_{\boldsymbol{P}} \left|\sigma_{ij}^{\alpha}(\boldsymbol{x}-\boldsymbol{P})\right| \propto \int^{\infty} dR\, 4\pi R^2 \frac{1}{R^2} \propto \int^{\infty} dR \sim \infty \tag{14}$$

Nevertheless, the second derivatives of the stress $\partial_k\partial_l\sigma_{ij}$ (with respect to the field coordinate) are proportional to $1/R^4$, and their sum is absolutely convergent. Therefore, the regularized periodic stress field $\boldsymbol{\sigma}^{\mathrm{reg}}$ is obtained by integration as:

$$\sigma_{ij}^{\mathrm{reg}}(\boldsymbol{x}) = \sigma_{ij}^{\mathrm{tot}}(\boldsymbol{x}) - \Theta_{ijk}x_k - \sigma_{ij}^{0} \tag{15}$$

where Θ_{ijk} is a constant third order tensor quantifying the linear error term, and σ_{ij}^{0} is the volume average of the stress field over the primary cell. The regularized stress $\sigma_{ij}^{\mathrm{reg}}$ is fully obtained by determining the Θ_{ijk} and σ_{ij}^{0} tensors. For a primary supercell of rectangular shape with lengths L_x, L_y, L_z, tensor Θ_{ijk} can be measured by evaluating the stress field at the edge of the cell, e.g.:

$$\begin{aligned}
\Theta_{ij1} &= \left[\sigma_{ij}\left(\frac{L_x}{2},0,0\right) - \sigma_{ij}\left(-\frac{L_x}{2},0,0\right)\right]/L_x \\
\Theta_{ij2} &= \left[\sigma_{ij}\left(0,\frac{L_y}{2},0\right) - \sigma_{ij}\left(0,-\frac{L_y}{2},0\right)\right]/L_y \\
\Theta_{ij3} &= \left[\sigma_{ij}\left(0,0,\frac{L_z}{2}\right) - \sigma_{ij}\left(0,0,-\frac{L_z}{2}\right)\right]/L_z
\end{aligned} \tag{16}$$

while σ_{ij}^{0} is directly obtained by numerical integration of the stress field over the entire simulation cell divided by the cell volume.

3.3. Absolutely convergent energy solution

Combining the preceding sections, a complete regularized solution for the elastic energy of a periodic dislocation network is obtained following the procedure illustrated in figure 1. We seek the elastic energy of an arbitrary closed dislocation network with physical core radius a_0, for which a direct evaluation of $E^{\mathrm{vol}}(a_0)$ using integral (12) is not computationally feasible. We propose the following procedure.

First, the energy of the network is evaluated by explicitly summing the analytical contribution associated with each segment pair using expressions (2)-(5).

This calculation is performed for three different values of the core radius, namely for the desired value a_0 and for two additional large values $a_1, a_2 \gg a_0$. With this, the energy values $E^{\text{seg}}(a_0)$, $E^{\text{seg}}(a_1)$, and $E^{\text{seg}}(a_2)$ are obtained.

Second, the elastic energy is evaluated using expression (12) by numerical integration of the stress field over the primary simulation cell for the two large values of the core radius a_1 and a_2 selected precedently. During this procedure, the stress is first evaluated at all integration points using relation (13). The error tensors Θ_{ijk} and σ^0_{ij} are then evaluated and the regularized stress field obtained from equation (15) is integrated. Obviously, the central idea of the method relies in selecting sufficiently large values of the core radius such that the numerical evaluation of $E^{\text{vol}}(a_1)$ and $E^{\text{vol}}(a_2)$ remains tractable.

The final step lies in the determination of the regularization constants E_0 and E_1 introduced in equation (11). On the one hand, the elastic energies $E^{\text{vol}}(a_1)$ and $E^{\text{vol}}(a_2)$ obtained from volume integral of the regularized stress are the unique energy values for their respective core radius values. On the other hand, from uniqueness of the energy content, both measures $E^{\text{vol}}(a)$ and $E^{\text{reg}}(a)$ must be equal for any given value of a. Consequently, the constants E_0 and E_1 can be determined by solving the following system of equations:

$$\begin{cases} E^{\text{vol}}(a_1) = E^{\text{seg}}(a_1) - E_1 a_1^2 - E_0 \\ E^{\text{vol}}(a_2) = E^{\text{seg}}(a_2) - E_1 a_2^2 - E_0 \end{cases} \tag{17}$$

and the unique regularized value of the network energy $E^{\text{reg}}(a_0)$ at desired core radius a_0 is obtained from relation (11) as:

$$E^{\text{reg}}(a_0) = E^{\text{seg}}(a_0) - E_1 a_0^2 - E_0 \tag{18}$$

4. Validation of the method

4.1. Glissile dislocation loop

As a first benchmark, our procedure is applied to calculate the elastic energy of a single glissile dislocation loop embedded in a periodic simulation cell. The loop has a radius $r = 100\,b$ and is positioned on a [001] plane at the center of a cubic primary cell of length $1000\,b$. The loop is discretized into 16 dislocation segments with Burgers vector $[b\,0\,0]$, where $b = 2.55 \times 10^{-10}$ m is the magnitude of the Burgers vector in FCC Cu.

For the calculation, we consider different values of the core width a ranging from $20\,b$ to $200\,b$, and different values of the number of periodic images $N^{\text{img}} = \{11, 21\}$ to be included in each direction. Note that in practice fewer periodic images N^{img} can be used; the large numbers of images considered here are only chosen to clearly illustrate the effects of the conditional convergence.

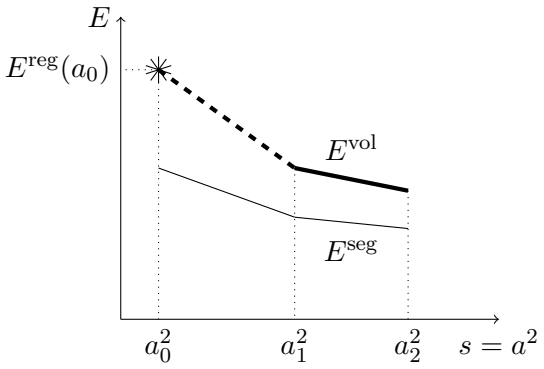

Figure 1: Schematic of the regularization procedure proposed to compute the elastic energy of a periodic dislocation network with core radius a_0. The energy of the network is first calculated from explicit segment pair interactions for three values of the core radius: a_0, and two large values $a_1, a_2 \gg a_0$ (thin line). The energy is then calculated by evaluating the volume integral of dislocation induced stresses for large core radius a_1 and a_2, for which the integration procedure remains tractable (solid thick line). Comparing both solutions, the correction terms E_0 and E_1 arising from the conditional convergence (see equation (11)) are determined and the regularized energy $E^{\mathrm{reg}}(a_0)$ is obtained (asterisk).

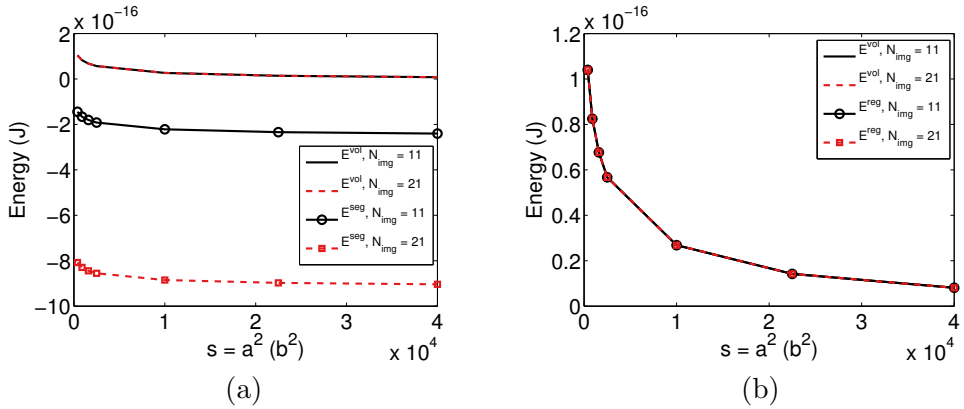

Figure 2: Elastic energy of a glissile dislocation loop as a function of the core parameter $s = a^2$ for different numbers of periodic images N_{img}. (a) Energies obtained from volume integration of the stress field (E^{vol}) and from explicit calculation of segment pairs interaction energies (E^{seg}). The values of E^{seg} depend on the number of periodic images, owing to the conditional convergent behavior. (b) Regularized energy E^{reg} obtained after applying the regularization procedure developed in this work.

Figure 2(a) shows the values for the elastic energy E^{seg} and E^{vol} computed using equations (3) and (12), respectively, as a function of the core radius a. First, it is shown that, as intended, the energy E^{vol} obtained by integration of

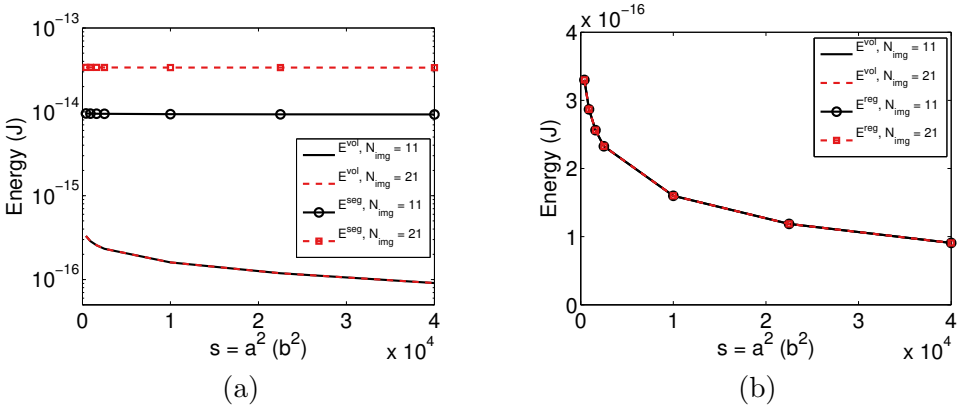

(a) (b)

Figure 3: Elastic energy of an infinite edge dislocation as a function of the core radius a for different numbers of periodic images N_{img}. (a) Energy obtained from volume integration of the stress field (E^{vol}) and from explicit calculation of segment pairs interaction energies (E^{seg}), plotted in semi-log scale. (b) Regularized energy E^{reg} obtained after applying the regularization procedure developed in this work.

the regularized stress field (see §3.2) does not depend on the number of periodic images used in the calculation, as long as N_{img} is large enough to reach convergence. On the other hand, it is observed that the elastic energy E^{seg} obtained by explicitly summing segment pairs interactions does not converge, owing to the conditionally convergent behavior discussed in §2.2. Specifically, the energies E^{seg} obtained for $N_{\text{img}} = 11$ and $N_{\text{img}} = 21$ both differ from the volume-based energy E^{vol} by a constant term that does not depend on the core radius a. This is because the net Burgers vector content vanishes for a volume containing a closed dislocation loop, thereby preserving the periodicity of the internal stress field across periodic cell replica. Consequently, the linear regularization term E_1 in equation (11) is null and the regularized energy solution E^{reg} only involves constant term E_0 in this case.

Following the regularization procedure summarized in §3.3, the correction term E_0 is obtained by solving system (17). This is done using the energies E^{seg} values calculated for two large core radius, i.e. $a_1 = 100\,b$ and $a_2 = 200\,b$. The regularized energies E^{reg} for $a < 100\,b$ are then obtained using equation (11) and are plotted in figure 2(b). As expected, the regularized loop energies perfectly match the elastic energy E^{vol} values obtained from volume integral of dislocation stresses for all values of core radius a, thereby validating our approach for individual closed dislocation loops.

4.2. Infinite edge dislocation

To complete the validation of our approach, we now consider the case of an infinite edge dislocation contained in a periodic simulation cell. The dislocation

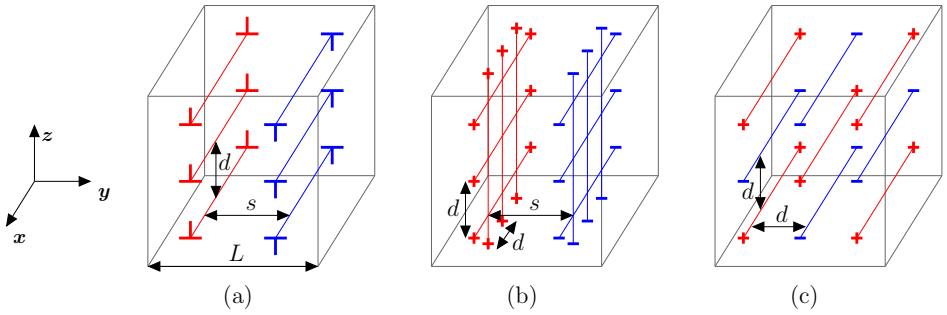

Figure 4: Schematic of the three types of ideal configurations considered. Plus (+) and minus (−) indicate the sign of the dislocation lines, which can have edge or screw characters. The configurations are periodic in all directions. (a) Low-angle tilt boundary dipole, composed of two arrays of edge dislocations with opposite Burgers vector. d denotes the dislocation spacing within each array, and s is the distance between both arrays. (b) Low-angle twist boundary dipole, composed of two arrays of crisscross screw dislocations. (c) Taylor lattice composed of a uniform 2D array of dislocations of alternating signs. Lattices entirely composed of edge or screw dislocations are considered.

line is aligned along the x-direction with Burgers vector in the y-direction. Unlike the previous example, the net Burgers vector is non-zero in the primary supercell for this setting. As a result, it is observed that the volume-based E^{vol} and interaction-based E^{tot} energies no longer differ by a constant term, but exhibit a (linear) dependence to the core parameter $s = a^2$, as shown in figure 3(a).

Regularized energies E^{reg} are obtained after determining the regularization constants E_0 and E_1 using equation (17) with $a_1 = 100\,b$ and $a_2 = 200\,b$. As reported in figure 3(b), the regularized energies here also perfectly match the values of the energy for all values of the core radius.

5. Applications and results

5.1. Grain-boundary arrays and Taylor lattices

Our approach is now applied to examine the elastic energy associated with idealized dislocation structures that play important roles in various continuum theories of plasticity. Namely, we consider the three classes of multipolar arrangements depicted in figure 4: (a) a pair of low-angle tilt boundaries, (b) a pair of low-angle twist boundaries, and (c) edge and screw Taylor lattices.

As illustrated in figure 4(a), the tilt boundary configuration is modeled with two arrays of edge dislocations, aligned along the x-direction, with opposite Burgers vectors, i.e. respectively pointing in the positive and negative y-directions. The dislocations are stacked in the z-direction with spacing d, and both arrays are separated by distance $s = L/2$, where L is the length of the primary volume $V = L^3$. The twist boundaries are composed of two sets of crisscross screw

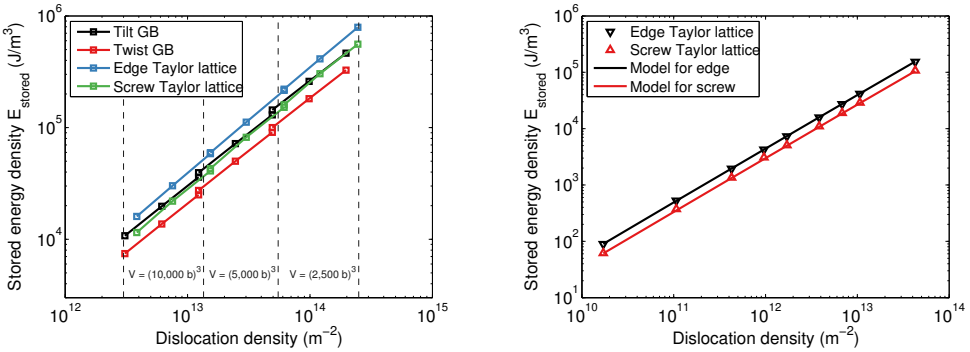

Figure 5: (a) Stored energy density E_{stored} for four types of multipolar arrangements as a function of the dislocation density ρ. The different density regions correspond to different primary volume sizes V, as indicated on the figure. (b) Stored energy density E_{stored} associated with pure edge and pure screw Taylor lattices as a function of the dislocation density ρ, compared to the simple model in equation (20).

dislocations, as depicted in figure 4(b). Each set is composed of two arrays of perpendicular screw dislocations aligned in the x- and z-directions, both with spacing d. Finally, the Taylor lattice consists in a two-dimensional array of infinite dislocations of alternating signs, aligned in the x-direction, and regularly spaced along the y- and z-directions, as illustrated in figure 4(c). We consider the cases of Taylor lattices entirely composed of edge and screw dislocations. For all configurations, periodicity is applied in all three spatial directions.

The regularized stored energy density $E_{\text{stored}} = E^{\text{reg}}/V$ calculated for these configurations using the approach presented in section 3 are reported in figure 5(a) for a wide range of dislocation density ρ. The different dislocation densities were produced by varying both the dislocations spacing d (i.e. the number of lines stacked on top of each other) and the primary simulation volume size V. The energies were calculated for a core radius value of $a_0 = 0.1b$, where $b = 2.55 \times 10^{-10}$ m is the magnitude of the Burgers vector in FCC Cu, and for shear modulus $\mu = 54.6$ GPa and Poisson's ratio $\nu = 0.324$.

Among all configurations, the results in figure 5(a) show that, at equivalent densities, the edge Taylor lattice has the higher elastic energy, while the stored energy of the twist boundary dipole is the lowest, consistent with the fact that the screw dislocation possesses the lowest energy of all possible characters. In addition, the screw Taylor lattice and tilt boundary dipoles are found to have similar energy content.

Importantly, it is also observed that the stored energy of all structures exhibit, when plotted on log-log scales, what appears to be a linear dependence on the dislocation density. In fact, for these simple configurations, this result is

consistent with the dislocation energy model found in the literature; considering the strain and stress fields of a single straight dislocation of length L, it can be shown that the elastic energy E per unit volume can be expressed as [17]:

$$E = A\frac{\mu b^2 L}{4\pi V}\ln\left(\frac{R}{a_0}\right) = A\frac{\mu b^2}{4\pi}\rho\ln\left(\frac{R}{a_0}\right) \tag{19}$$

where $A = 1$ for screw and $A = 1/(1-\nu)$ for edge dislocations, and R is the outer cut-off radius for the dislocation stress field. Essentially, equation (19) indicates that the dislocation energy possesses a linear dependence on the density, and a logarithmic term that depends on the interaction range. When several dislocations are present in the volume, it is often assumed that the outer cut-off R is related to the dislocation geometric mean spacing, i.e. $R \propto 1/\sqrt{\rho}$, such that the stored energy density in equation (19) is given as:

$$E = A\frac{\mu b^2}{4\pi}\rho\ln\left(\frac{1}{a_0\sqrt{\rho}}\right) \tag{20}$$

The validity of this relation is examined by comparing equation (20) with the stored energy calculated using our approach for edge and screw Taylor lattices. The results reported in figure 5(b) show an excellent agreement between the model and the calculations over a large range of dislocation densities. Clearly, this agreement results from the fact that the spacing between neighboring dislocation lines is indeed on the order $1/\sqrt{\rho}$ in the Taylor lattice, and the stress fields of dislocations entirely cancel out beyond this distance due to the uniform multipolar arrangement. The excellent agreement between equation (20) and the numerically evaluated energy of the Taylor lattices is significant because the energy depends not only on the dislocation density but also on dislocations arrangement. For example, we see that the energies of tilt and twist boundaries do not follow equation (20). However, we will show in the next section that equation (20) generalizes surprisingly well for large-scale, complex networks of dislocations produced during work-hardening simulations.

5.2. Large-scale discrete dislocation networks

In this section, our approach is used to calculate the stored energy associated with large dislocation networks generated during a DDD simulation of work-hardening, for which an example is shown in figure 6(a). To obtain such networks, a $(15\mu\text{m})^3$ FCC copper periodic configuration made of infinite straight lines randomly distributed on $\{1\,1\,1\}$ planes is first relaxed to an equilibrium state, giving an initial dislocation density $\rho_0 = 0.7 \times 10^{12}$ m^{-2}. The configuration is then subjected to a constant strain rate $\dot{\epsilon} = 10^3$ s^{-1} along the $[0\,0\,1]$ direction up to $\gamma = 1.2\%$ shear strain. The simulations were performed using the ParaDiS program [18] and the recently developed subcycling integrator [19].

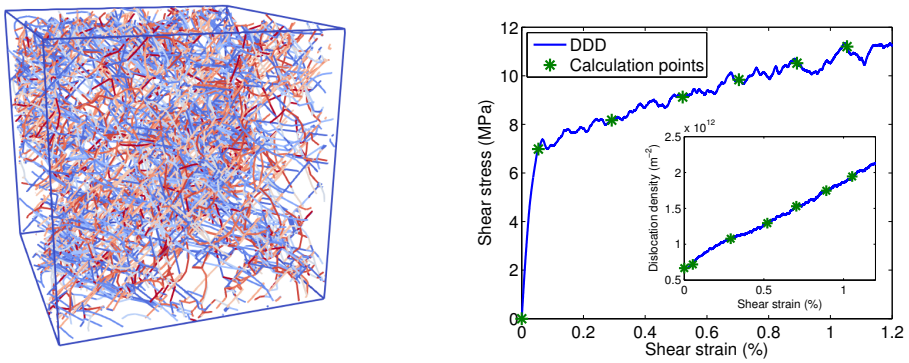

(a) (b)

Figure 6: (a) Snapshot of a DDD periodic $(15\mu\text{m})^3$ dislocation network loaded at $\gamma \approx 1\%$ shear strain along the [0 0 1] direction. Dislocation lines are colored by slip systems. (b) Shear stress-strain curves and dislocation density predicted by the DDD work-hardening simulation (blue lines). The different DDD configurations for which the elastic energy was calculated at various levels of the deformation are indicated with green asterisks.

The shear stress-strain curves and dislocation density evolution predicted by the DDD simulation are reported in figure 6(b). During loading, the total work W done to the crystal (per unit volume) is given by:

$$W(\gamma) = \frac{1}{2}\int_0^{\gamma} \varepsilon(u)\sigma(u)du \tag{21}$$

where $\varepsilon = S\gamma$ and $\sigma = \tau/S$ are the normal strain and stress along the loading direction, related to the shear stress-strain curve shown in figure 6(b) through the Schmid factor $S \approx 0.41$.

To investigate the evolution of the dislocations energy during deformation, the stored energy was calculated for several configurations obtained at different levels of deformation, whose strains are marked with asterisks in the curves shown in figure 6(b). Specifically, the incremental stored energy ΔE_{stored} for these configurations was calculated as:

$$\Delta E_{\text{stored}}(\gamma) = E_{\text{stored}}(\gamma) - E_{\text{stored}}(0) \tag{22}$$

where $E_{\text{stored}}(0)$ is the regularized elastic energy associated with the initial, relaxed configuration with density ρ_0. In order to compare our calculations with experimental results, we now include a core energy contribution in the calculation of the stored energies in equation (22). As detailed in Appendix C, the core energy term is informed from atomistic simulations, and allows to eliminate the dependence of the elastic energy on the choice of the core radius a_0.

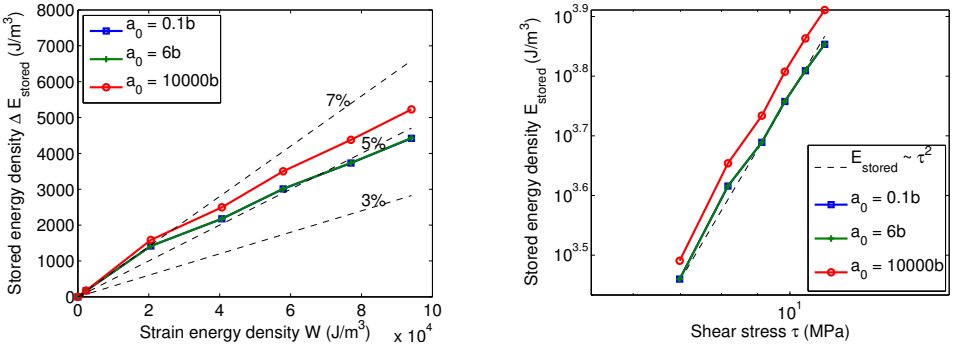

Figure 7: (a) Evolution of the stored elastic energy ΔE_{stored} in the dislocation network as a function of the total work done per unit volume W during loading, for different values of the core radius a. Our DDD simulation predicts that approximately 5% of the expended work is stored in the dislocation network. (b) Stored energy E_{stored} as a function of the shear stress τ on a log-log scale plot. The relation $E_{\text{stored}} \propto \tau^2$ is well obeyed.

Figure 7(a) reports the evolution of the stored elastic energy ΔE_{stored} in the dislocation networks as a function of the expended work W during loading. The energies are calculated for different values of the core radius a_0 using $N_{\text{img}} = 3$ periodic images in each direction. Results obtained for physically consistent values of the core radius (i.e. $a_0 = 0.1b$ and $a_0 = 6b$) show that the fraction $p = W/\Delta E_{\text{stored}}$ of the stored energy to total work amounts to about 5% on the range $\gamma = 0$ to 1% shear strain. This result is in good agreement with the value of $6 - 7\%$ measured experimentally on Cu single-crystals [4, 5] and predicted by the theory [9] during stage II hardening. In addition, the instantaneous stored energy E_{stored} dependence on the shear stress τ is found to agree very well with the quadratic relation $E_{\text{stored}} \propto \tau^2$ proposed in the literature [4, 5], as attested by the results shown in figure 7(b).

The evolution of the instantaneous stored energy E_{stored} as a function of the dislocation density ρ is also reported in figure 8, during both the initial relaxation and the loading regime. As expected, the unrelaxed configuration made of straight lines first reduces its internal energy during the relaxation step. This is primarily achieved via the formation of dislocation junctions, which is accompanied by a slight decrease in the dislocation density. During this process, the stored energy is found to rapidly drop and settle within the bounds set by the energy model in equation (20) for Taylor lattices consisting of pure edge and pure screw dislocations. Remarkably, it is then observed that, during loading, the energy of the complex DDD networks remains well within the bounds of the model for edge and screw orientations. Clearly, one should not expect the stored energy to match the model for either one of these characters, as the strain-

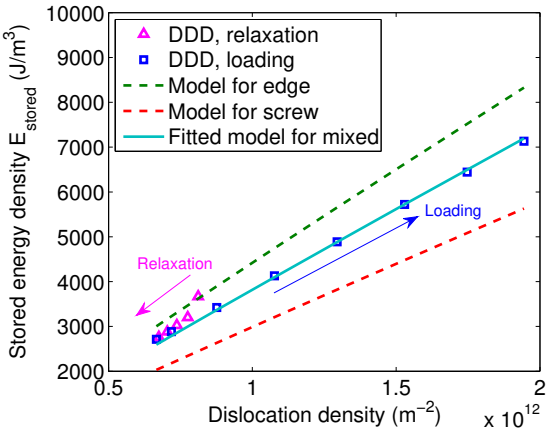

Figure 8: Evolution of the stored energy E_{stored} as a function of the dislocation density ρ during initial relaxation and loading, compared to the model in equation (20) for pure edge and pure screw dislocations. A very good agreement is obtained when fitting the dislocation character coefficient A in equation (20) to the DDD results during loading (i.e. considering mixed character). The best fit is obtained for $A^{\text{fit}} = 1.278$, i.e. corresponding to an average dislocation orientation of $\theta = 49.6°$.

hardened dislocation networks are primarily composed of dislocation of mixed characters found in complex arrangements, as shown in figure 6(a). However, a very good agreement is obtained if we consider the Taylor lattice of mixed dislocations. This can be simply achieved by treating the character-dependent coefficient A in equation (20) as a fitting parameter to the DDD stored energy results. For reference, the best fit with $A^{\text{fit}} = 1.278$ obtained by the least-square method is reported in figure 8. If we assume that the line energy continuously varies from screw to edge characters, A can be expressed as $A(\theta) = \cos^2\theta + 1/(1-\nu)\sin^2\theta$, where θ is the character angle between dislocation lines and their Burgers vector. Interestingly, the fitted value of A^{fit} corresponds to an effective dislocation orientation of $\theta = 49.6°$, in very close agreement with the average dislocation line orientation of $\theta = 49.7°$ which is found to be nearly constant during the DDD simulation.

6. Discussion

6.1. Taylor hardening and dislocation screening

As shown numerically in section 5.1, the simple energy model in equation (20) provides an excellent description of the energy associated with Taylor lattices. Concurrently, we also found in section 5.2 that the stored energy in complex networks generated by work-hardening simulations can be well described when the

simple model considers a collection of mixed dislocations with some average character angle. Together, these results suggest that a Taylor lattice model composed of dislocations of mixed character is able to capture very well the energetics of complex structures produced during work-hardening.

This finding is surprising because the two dislocation structures are very different. On the one hand, strain-hardened structures form intricate networks of dislocation links connected to one another through dislocation junctions. The complexity of such networks further manifests in that dislocation links are found in a wide range of orientations, and their lengths closely follow an exponential distribution [13]. On the other hand, the Taylor lattice is formed by infinitely long, straight and parallel dislocation lines, which are uniformly spaced and unconnected to each other. Yet, despite its simplicity and its topology that is far from real dislocation structures, such an idealized configuration provides an accurate model for the stored energy associated with intricate dislocation networks, and seems to act as an "attractor" for the evolution of the microstructure energetics.

From a general perspective, this finding helps to explain the success of the Taylor hardening model [1],

$$\tau = \alpha \mu b \sqrt{\rho}\,, \tag{23}$$

which relates the flow stress to the dislocation density, via the interaction strength coefficient $\alpha \approx 0.5 - 1$ [20]. In fact, the Taylor model was originally derived by considering Taylor lattices (see figure 4(c)) formed by straight, parallel dislocation lines whose nearest neighbor spacing is on the order $1/\sqrt{\rho}$. Subsequently, it has been interpreted as the critical stress required to activate dislocation lines, whose average length between pinning points in physical networks is on the order of the mean spacing of $\lambda = 1/\sqrt{\rho}$. The fact that the stored energy of strain-hardened networks is found to be well described by the energy associated with Taylor lattices suggests that, despite resulting from heterogeneous dislocation distributions with complex spatial arrangements, the long-range stresses tend to cancel out beyond distance λ. This observation is important for two reasons: (i) it reinforces the hypothesis that work-hardening is primarily controlled by short-range interactions, e.g. junction formation, whose key role has been consistently demonstrated using DDD simulations [12, 13], (ii) it shows that the network structure evolves in such a way that the stress fields are screened at distances beyond $1/\sqrt{\rho}$.

Interestingly, this finding of stress field screening is consistent with X-ray diffraction line analysis. In the diffraction theory, the diffraction peaks widths diverge logarithmically with the crystal size if dislocations were randomly distributed [21]. Realizing that the divergence of X-ray broadening is of the same kind as the divergence of the elastic energy, Wilkens proposed a *randomly restricted* distribution, where dislocations arrange in sub-regions in which their

total strain field is entirely contained [22]. In an analogous manner to the cut-off radius R introduced in equation (19), the size of the sub-regions in the *randomly restricted* distribution is associated with a correlation length R_c that quantifies the screening of stresses and strains by neighboring dislocations. By fitting to experimental diffraction peaks, correlation lengths R_c with values ranging between 1 and 3 times the mean dislocation spacing λ were obtained [23, 24], confirming that dislocations are strongly correlated in real crystals. Subsequently, the screening of dislocations stress was examined numerically in detail by considering idealized edge and screw dislocations distributions in two dimensions [25, 26], and analytical calculations based on the analysis of energy functionals in the presence of excess dislocation density were proposed [27, 28], providing direct evidences for stress screening. Here we show that dislocation screening naturally arises in complex three-dimensional structures produced during strain hardening simulations, which is consistent with experimental X-ray results and stress screening analyses.

6.2. Consistency and robustness of the numerical approach

The numerical method presented in this work relies on the non-singular formulation to evaluate the dislocation energy content. While the evaluation of the elastic energy readily depends on the choice of the core radius a_0, this arbitrariness is formally eliminated by including a core energy term in the calculation of the total dislocation energy (see Appendix C). Alternatively, the core radius could be simply treated as a fitting parameter to be calibrated against the experimental data (and the core energy would no longer be included). However, such an approach would not allow us to assess the quality of DDD predictions, but would rather provide an estimate of the effective core value a_0 associated with DDD models. Therefore, we believe that including a core energy whose contribution is informed from atomistic simulations is a more relevant approach towards accurately evaluating dislocation energies from DDD configurations. In addition, we note that the core contribution is not subjected to the issue of conditional convergence. Therefore, it does not need to be included in the regularization procedure developed in section 3, but only needs to be added to the regularized elastic energy obtained at desired core radius a_0.

Results provided in figures 7(a)-(b) show the robustness and consistency of our method with respect to the values chosen for the core radius when adopting the core energy partitioning. Specifically, it is shown that the calculation performed with different but physically reasonable values for the core radius, namely $a_0 = 0.1\,b$ and $a_0 = 6\,b$, lead to the same values for the stored energies. This is because part of the elastic energies is transferred to the core contribution as the core parameter is being increased (see Appendix C). However, when the value for the core radius is exceedingly large, e.g. $a_0 = 10,000\,b$, it is observed that the

resulting stored energy is overestimated, as reported in figure 7(a). This result follows from the fact that, for very large values of the core radius, the stress fields of dislocation segments become so smeared out that the energy is almost exclusively accounted for by the core contribution. This observation is important as it shows that, despite its logarithmic contribution, the energy associated with short-range interactions is not negligible. In other words, the total energy of complex dislocation networks cannot be accurately estimated by solely considering the core energy. Otherwise, the energy would only depend on the dislocation density and not on the dislocation arrangement, which is known to be incorrect. This is why the rigorous numerical approach developed in this work to compute the dislocation energy is needed.

7. Conclusion

In this paper, we presented a method to evaluate the elastic energy associated with arbitrary three-dimensional dislocation networks subjected to periodic boundary conditions. The proposed approach addresses simultaneously the two main difficulties that are involved in such a calculation, namely (i) the conditional convergent behavior arising from the periodic sum of interaction energies, (ii) the computational cost associated with the numerical evaluation of the volume integral of dislocations stresses. The central idea of the approach consists in taking advantage of the non-singular theory of dislocations so as to treat the core radius as a numerical parameter. Exploiting the property that the periodic sum of the second derivative of the energy with respect to the core parameter converges at a sufficiently rapid rate, a regularized solution for the periodic interaction energies can be conveniently obtained. In this procedure, regularization constants are determined by comparing the interaction energy contributions summed explicitly with the energy obtained by volume integration of dislocations stress fields evaluated for two arbitrary, distinct values of the core radius. In particular, choosing large values for the core radius produces smooth stress fields that can be numerically integrated using a manageable number of integration points, thereby limiting the computational burden associated with such a calculation.

Using our approach, we found that the simple dislocation energy model proposed in the literature (see equation (20)) yields an excellent agreement with the internal elastic energy associated with (i) Taylor lattice arrangements of mixed dislocations, and with (ii) complex networks generated with DDD simulations. These results suggest that, in strain-hardened networks, long-range stresses are well screened at distances larger than the mean dislocation spacing. This finding is consistent with experimental X-ray diffraction line analysis, and helps to explain the success of the Taylor hardening model. In addition, we showed that the stored energies predicted by DDD simulations during multi-slip hardening

are consistent with the values measured experimentally, at about 5% of the work done.

In summary, the numerical approach proposed in this work offers an accurate and tractable technique to calculate the stored energy associated with periodic dislocation networks of arbitrary complexity, thereby enabling a direct comparison between stored energies predicted by DDD simulations with energies obtained from atomistic simulations and experiments.

Acknowledgement

This work was supported by the U.S. Department of Energy, Office of Basic Energy Sciences, Division of Materials Sciences and Engineering under Award No. DE-SC0010412.

Appendix A. Non-singular dislocation core distribution

Following the non-singular theory of dislocations proposed in [15], the singularity at the dislocation core appearing in the classical theory of elasticity can be eliminated by replacing the delta function description of the Burgers vector with a smooth density distribution function. Specifically, by spreading the Burgers vector using a well chosen isotropic core distribution $\tilde{\omega}(\boldsymbol{x}, a)$, a non-singular radius vector R_a can be conveniently obtained as:

$$R_a(\boldsymbol{x}) = R(\boldsymbol{x}) * \omega(\boldsymbol{x}, a) = \sqrt{R(\boldsymbol{x})^2 + a^2} = \sqrt{(x_i - x_i')(x_i - x_i') + a^2} \qquad \text{(A.1)}$$

where a denotes the core width parameter, $\omega(\boldsymbol{x}, a) = \tilde{\omega}(\boldsymbol{x}, a) * \tilde{\omega}(\boldsymbol{x}, a)$ is the convolution of the core distribution with itself, and $R = \|\boldsymbol{x} - \boldsymbol{x'}\|$ is the original radius vector, linking field point $\boldsymbol{x}$ to the coordinate $\boldsymbol{x'}$ spanning the dislocation segment. It can be shown that the distribution function leading to the expression of R_a in (A.1) is given by:

$$\omega(\boldsymbol{x}, a) = \frac{15}{8\pi a^3 \left[(r/a)^2 + 1\right]^{7/2}}, \quad r = \|\boldsymbol{x}\| \qquad \text{(A.2)}$$

The form of R_a conveniently implies that its derivatives follow the original expressions for those of R, e.g.:

$$
\begin{aligned}
R_{a,i} &= -\frac{R_i}{R_a} \\
R_{a,ij} &= \left(\delta_{ij} - \frac{R_i}{R_a}\frac{R_j}{R_a}\right)/R_a \\
R_{a,ijk} &= \left[-3\frac{R_i}{R_a}\frac{R_j}{R_a}\frac{R_k}{R_a} + \left(\delta_{ij}\frac{R_k}{R_a} + \delta_{jk}\frac{R_i}{R_a} + \delta_{ki}\frac{R_j}{R_a}\right)\right]/R_a^2
\end{aligned} \tag{A.3}
$$

where δ_{ij} is the Kronecker symbol.

Appendix B. Non-singular dislocation stress field

From the classical elasticity theory, the stress field at point $\boldsymbol{x}$ induced by a dislocation loop C with Burgers vector $\boldsymbol{b}$ in an infinite elastically isotropic medium is given in [29] by

$$
\begin{aligned}
\hat{\sigma}_{ij}(\boldsymbol{x}) = \frac{\mu b_n}{8\pi}\oint_C \Bigg[& R_{,mpp}\left(e_{jmn}dx'_i + e_{imn}dx'_j\right) \\
& + \frac{2}{1-\nu}e_{kmn}\left(R_{,ijm} - \delta_{ij}R_{,ppm}dx'_k\right)\Bigg]
\end{aligned} \tag{B.1}
$$

where e_{ijk} is the permutation tensor, $R_{,ijk} = \partial_i\partial_j\partial_k R$ are the third derivatives of the radius vector, and μ and ν are the shear modulus and Poisson's ratio of the medium, respectively.

In the context of the non-singular formulation, the non-singular stress field $\sigma_{ij}(\boldsymbol{x})$ is obtained by spreading the Burgers vector along the dislocation line, i.e. by taking the convolution of the singular stress field expressed in (B.1) with the core distribution function $\tilde{\omega}$ introduced in Appendix A, i.e.:

$$
\sigma_{ij}(\boldsymbol{x}) = \hat{\sigma}_{ij}(\boldsymbol{x}) * \tilde{\omega}(\boldsymbol{x}, a) \tag{B.2}
$$

No analytical form is available for $\tilde{\omega}(\boldsymbol{x}, a)$, hence no analytical expression is readily available for $\sigma_{ij}(\boldsymbol{x})$. However, the core distribution function is well approximated by the following expression [15]:

$$
\tilde{\omega}(\boldsymbol{x}, a) = 0.3425 \times \omega(\boldsymbol{x}, 0.9038a) + 0.6575 \times \omega(\boldsymbol{x}, 0.5451a) \tag{B.3}
$$

where $\omega(\boldsymbol{x}, a)$ is the self-convolution of $\tilde{\omega}(\boldsymbol{x}, a)$ whose analytical expression is provided in equation (A.2). Therefore, the non-singular stress field induced by a dislocation segment can be calculated by evaluating the doubly convoluted non-singular stress twice using two different values of the core radius and the weights

given in (B.3). For a dislocation segment α with Burgers vector $\boldsymbol{b}$ and end points at coordinates $\boldsymbol{x}_\alpha^1$ and $\boldsymbol{x}_\alpha^2$, the doubly convoluted stress at point $\boldsymbol{x}$ is given by:

$$\hat{\sigma}_{ij}(\boldsymbol{x}) * \omega(\boldsymbol{x}, a) = \frac{\mu b_n}{8\pi} \int_{\boldsymbol{x}_\alpha^1}^{\boldsymbol{x}_\alpha^2} \Big[R_{a,mpp} \left(e_{jmn} dx_i' + e_{imn} dx_j' \right) + \frac{2}{1-\nu} e_{kmn} \left(R_{a,ijm} - \delta_{ij} R_{a,ppm} dx_k' \right) \Big] \tag{B.4}$$

for which an analytical expression for straight dislocation segments is provided in [15].

Appendix C. Core energy partitioning

In the classical theory of elasticity, the elastic energy (per unit length) of a straight dislocation segment is given from equation (19) as [17]:

$$E^{\mathrm{el}}(a_0) = \frac{\mu b^2}{4\pi} \left(\cos^2\theta + \frac{\sin^2\theta}{1-\nu} \right) \ln\left(\frac{R}{a_0} \right) \tag{C.1}$$

where θ is the angle between the dislocation line and its Burgers vector $\boldsymbol{b}$, R is the outer radius describing the extent of the dislocation stress field, and a_0 is the inner core radius introduced to eliminate the singularly at the dislocation core.

Given the arbitrariness of a_0, the energy E^{el} in equation (C.1) does not correspond to a physically measurable quantity. To fix this issue, a core energy contribution E^{core} is typically introduced, such that the total energy of the dislocation line is decomposed as:

$$E^{\mathrm{tot}} = E^{\mathrm{el}}(a_0) + E^{\mathrm{core}}(a_0) \tag{C.2}$$

This partitioning is physically motivated by the fact that the elasticity theory does not apply in the dislocation core. In the context of the non-singular formulation, the core energy E^{core} can be regarded as a correction term introduced to make the total dislocation energy E^{tot} independent of the choice of the core radius a_0. Core energies can be calculated from the total dislocation energy obtained from *ab-initio* or atomistic simulations [16, 30–32], after the elastic part is removed following the partitioning in equation (C.2). For a core radius $a_0 = b$, the core energies typically amount to several tenths of one eV $\mathrm{\AA}^{-1}$ in FCC metals.

Since the values of the core energies are expected to depend on the character of the dislocation line, it is often assumed that the core contribution takes the same form as the elastic energy, i.e.

$$E^{\mathrm{core}}(a_0) = \frac{\mu b^2}{4\pi} \left(\sin^2\theta + \frac{\cos^2\theta}{1-\nu} \right) \ln\left(\frac{a_0}{r_0} \right) \tag{C.3}$$

This form of the core energy is typically used in DDD codes in which the partitioning in equation (C.2) is adopted, such as in the ParaDiS code [18]. In equation (C.3), r_0 is an additional core parameter, whose value is fitted such that expression (C.3) match the core contribution determined with atomistic models, e.g.:

$$r_0 = a_0 \exp\left(-\frac{E_{\mathrm{s}}^{\mathrm{core}}(a_0)\,4\pi}{\mu b^2}\right) \tag{C.4}$$

where $E_{\mathrm{s}}^{\mathrm{core}}(a_0)$ is the core energy (per unit length) obtained at radius a_0 for screw dislocations. Values of $E_{\mathrm{s}}^{\mathrm{core}}$ ranging in $0.3 - 0.5\,\mathrm{eV\,\AA^{-1}}$ obtained at $a_0 \approx b$ from atomistic simulations in various metals [16, 30, 32] suggest that $r_0 = 0.1\,b$ is a reasonable choice to describe the core contribution. This value for the core parameter r_0 is also consistent with the core energy estimate $E_{\mathrm{s}}^{\mathrm{core}} \approx \mu b^3/3 \approx 0.7\,\mathrm{eV\,\AA^{-1}}$ at $a_0 = 1\,\mathrm{nm}$ proposed in [33]. Hence we use this value to compare our calculations with experimental energy measurements in §5.2. (Note that $r_0 = 0.1\,b$ is the default value used in ParaDiS [18] to compute the core energy.)

Despite its physical motivation, the partitioning introduced in equation (C.2) is artificial in that the relative contributions of the elastic and core terms depend on the value chosen for the core radius a_0. Here we point out that, in the context of the non-singular formulation, the value chosen for a_0 to accurately evaluate the total energy of a dislocation network must nonetheless remain consistent with the physical size of the dislocation core, e.g. in the range of $0.1\,b$ to $10\,b$. This is because when several dislocations are present, the elastic energy is strongly governed by lines interactions. Since choosing a very large value for a_0 results in transferring most of the energy to the core contribution, the elastic interactions contribution is effectively weakened, which is unphysical.

As discussed in section 6, the effect of the choice of the core radius a_0, when using the partitioning in equation (C.2), is well illustrated in the results reported in figure 7(a). It is observed that results for the stored energy are very consistent when using physically reasonable values $a_0 = 0.1\,b$ and $a_0 = 6\,b$ for the core radius, while the energy is overestimated when a very large value of $a_0 = 10000\,b$ is used. (Note that the core energy contribution is null for $a_0 = r_0 = 0.1\,b$.) This observation is important as it indicates that (i) the energy of a dislocation network cannot be accurately estimated by considering a collection of isolated lines, i.e. interaction energies cannot be neglected, and (ii) quantifying the stored energy of dislocation networks therefore requires an accurate, yet tractable calculation method such as that developed in this work.

References

[1] G. I. Taylor, The Mechanism of Plastic Deformation of Crystals. Part I. Theoretical, Vol. 145, 1934.

[2] M. Bever, D. Holt, A. Titchener, The stored energy of cold work, Progress in Materials Science 17 (1973) 5 – 177.
[3] D. Kuhlmann-Wilsdorf, Theory of workhardening 1934-1984, Metallurgical Transactions A 16 (12) (1985) 2091–2108.
[4] H. Steffen, G. Gottstein, H. Wollenberger, Stored energy measurements in copper single crystals tensile deformed at 20c, Acta Metallurgica 21 (5) (1973) 683 – 689.
[5] G. Gottstein, J. Bewerunge, H. Mecking, H. Wollenberger, Stored energy of 78 k tensile deformed copper crystals, Acta Metallurgica 23 (5) (1975) 641 – 652.
[6] D. Ronnpagel, C. Schwink, Measurement of the stored energy of copper single crystals by means of a new deformation calorimetry method, Acta Metallurgica 26 (2) (1978) 319 – 331.
[7] J.-L. Chaboche, Cyclic viscoplastic constitutive equations, part ii: Stored energycomparison between models and experiments, Journal of Applied Mechanics 60 (4) (1993) 822–828.
[8] P. Rosakis, A. Rosakis, G. Ravichandran, J. Hodowany, A thermodynamic internal variable model for the partition of plastic work into heat and stored energy in metals, Journal of the Mechanics and Physics of Solids 48 (3) (2000) 581 – 607.
[9] A. Seeger, H. Kronmller, Stored energy and recovery of deformed f.c.c. metals, The Philosophical Magazine: A Journal of Theoretical Experimental and Applied Physics 7 (78) (1962) 897–913.
[10] V. Berdichevsky, Energy of dislocation networks, International Journal of Engineering Science 103 (2016) 35 – 44.
[11] A. Benzerga, Y. Bréchet, A. Needleman, E. V. der Giessen, The stored energy of cold work: Predictions from discrete dislocation plasticity, Acta Materialia 53 (18) (2005) 4765 – 4779.
[12] V. V. Bulatov, L. L. Hsiung, M. Tang, A. Arsenlis, M. C. Bartelt, W. Cai, J. N. Florando, M. Hiratani, M. Rhee, G. Hommes, T. G. Pierce, T. D. de la Rubia, Dislocation multi-junctions and strain hardening, Nature 440 (7088) (2006) 1174–1178.
[13] R. B. Sills, N. Bertin, A. Aghaei, W. Cai, Dislocation Networks and the Microstructural Origin of Strain Hardening, ArXiv e-printsarXiv:1712.00120.
[14] R. LeSar, Ambiguities in the calculation of dislocation self energies, physica status solidi (b) 241 (13) (2004) 2875–2880.
[15] W. Cai, A. Arsenlis, C. R. Weinberger, V. V. Bulatov, A non-singular continuum theory of dislocations, Journal of the Mechanics and Physics of Solids 54 (3) (2006) 561–587.
[16] W. Cai, V. V. Bulatov, J. Chang, J. Li, S. Yip, Periodic image effects in dislocation modelling, Philosophical Magazine 83 (5) (2003) 539–567.
[17] D. Hull, D. Bacon, Introduction to Dislocations (Fifth Edition), Butterworth-Heinemann, Oxford, 2011.
[18] A. Arsenlis, W. Cai, M. Tang, M. Rhee, T. Oppelstrup, G. Hommes, T. G. Pierce, V. V. Bulatov, Enabling strain hardening simulations with dislocation dynamics, Modelling and Simulation in Materials Science and Engineering 15 (6) (2007) 553–595.
[19] R. B. Sills, A. Aghaei, W. Cai, Advanced time integration algorithms for dislocation dynamics simulations of work hardening, Modelling and Simulation in Materials Science and Engineering 24 (4) (2016) 045019.
[20] H. Mecking, U. F. Kocks, Kinetics of flow and strain-hardening, Acta Metallurgica 29 (11) (1981) 1865–1875.
[21] M. Krivoglaz, K. P. Ryaboshapka, Theory of x-ray scattering by crystals containing dislocations, screw and edge dislocations randomly, Fiz. Metallov. Metalloved 15 (1963) 18–31.
[22] M. Wilkens, The determination of density and distribution of dislocations in deformed single crystals from broadened x-ray diffraction profiles, Physica status solidi (a) 2 (2) (1970) 359–370.
[23] T. Ungar, H. Mughrabi, D. Rönnpagel, M. Wilkens, X-ray line-broadening study of the dislocation cell structure in deformed [001]-orientated copper single crystals, Acta Metal-

lurgica 32 (3) (1984) 333–342.
[24] T. Ungár, J. Gubicza, G. Ribárik, A. Borbély, Crystallite size distribution and dislocation structure determined by diffraction profile analysis: principles and practical application to cubic and hexagonal crystals, Journal of Applied Crystallography 34 (3) (2001) 298–310.
[25] J.-D. Kamminga, R. Delhez, Calculation of diffraction line profiles from specimens with dislocations. A comparison of analytical models with computer simulations, Journal of Applied Crystallography 33 (4) (2000) 1122–1127.
[26] V. M. Kaganer, K. K. Sabelfeld, X-ray diffraction peaks from correlated dislocations: Monte carlo study of dislocation screening, Acta Crystallographica Section A: Foundations of Crystallography 66 (6) (2010) 703–716.
[27] I. Groma, G. Györgyi, B. Kocsis, Debye screening of dislocations, Physical review letters 96 (16) (2006) 165503.
[28] M. Zaiser, Local density approximation for the energy functional of three-dimensional dislocation systems, Physical Review B 92 (17) (2015) 174120.
[29] T. Mura, Micromechanics of Defects in Solids, Martinus Nijhoff, Dordrecht, 1982.
[30] W. Cai, V. V. Bulatov, J. Chang, J. Li, S. Yip, Anisotropic elastic interactions of a periodic dislocation array, Phys. Rev. Lett. 86 (2001) 5727–5730.
[31] E. Clouet, L. Ventelon, F. Willaime, Dislocation core energies and core fields from first principles, Phys. Rev. Lett. 102 (2009) 055502.
[32] X. W. Zhou, R. B. Sills, D. K. Ward, R. A. Karnesky, Atomistic calculations of dislocation core energy in aluminium, Phys. Rev. B 95 (2017) 054112.
[33] A. H. Cottrell, Dislocations and Plastic Flow in Crystals, Oxford University Press, Fair Lawn, N.J., 1953.